sustainability

MDPI

Article

Techno-Economic Assessment of the Supercritical Carbon Dioxide Enhanced Geothermal Systems

Mauro Tagliaferri [1], Paweł Gładysz [2,*], Pietro Ungar [1], Magdalena Strojny [2], Lorenzo Talluri [1], Daniele Fiaschi [1], Giampaolo Manfrida [1], Trond Andresen [3] and Anna Sowiżdżał [4]

[1] Department of Industrial Engineering, University of Florence, 50121 Firenze, Italy
[2] Faculty of Energy and Fuels, AGH University of Science and Technology, 30-059 Kraków, Poland
[3] SINTEF Energy Research, 7034 Trondheim, Norway
[4] Faculty of Geology, Geophysics and Environmental Protection, AGH University of Science and Technology, 30-059 Kraków, Poland
* Correspondence: pawel.gladysz@agh.edu.pl

Abstract: Enhanced geothermal systems distinguish themselves among other technologies that utilize renewable energy sources by their possibility of the partial sequestration of carbon dioxide (CO_2). Thus, CO_2 in its supercritical form in such units may be considered as better working fluid for heat transfer than conventionally used water. The main goal of the study was to perform the techno-economic analysis of different configurations of supercritical carbon dioxide-enhanced geothermal systems (sCO_2-EGSs). The energy performance as well as economic evaluation including heat and power generation, capital and operational expenditures, and levelized cost of electricity and heat were investigated based on the results of mathematical modeling and process simulations. The results indicated that sCO_2 mass flow rates and injection temperature have a significant impact on energetic results and also cost estimation. In relation to financial assessment, the highest levelized cost of electricity was obtained for the indirect sCO_2 cycle (219.5 EUR/MWh) mainly due to the lower electricity production (in comparison with systems using Organic Rankine Cycle) and high investment costs. Both energy and economic assessments in this study provide a systematic approach to compare the sCO_2-EGS variants.

Keywords: enhanced geothermal systems; CO_2-EGS; supercritical carbon dioxide cycles; Organic Rankine Cycle; combined heat and power; geothermal energy

Citation: Tagliaferri, M.; Gładysz, P.; Ungar, P.; Strojny, M.; Talluri, L.; Fiaschi, D.; Manfrida, G.; Andresen, T.; Sowiżdżał, A. Techno-Economic Assessment of the Supercritical Carbon Dioxide Enhanced Geothermal Systems. *Sustainability* **2022**, *14*, 16580. https://doi.org/10.3390/su142416580

Academic Editor: Kian Jon Chua

Received: 21 September 2022
Accepted: 2 December 2022
Published: 10 December 2022

1. Introduction

In recent years, energy problems and global warming have become the most discussed issues by countries around the world. An economic system increasingly sensitive to the environment, the search for energy independence, and the development of an industrial sector highly dependent on electricity are just a few causes that have pushed the European Union (EU) to adopt drastic changes in European energy production and global electricity grid. The increase in the energy produced through renewable systems represents the main objective in order to be able to face the energetic and environmental requirements determined in the conference in Paris in 2020. In accordance with future goals, The European Commission is seeking to accelerate the take-up of renewables in the EU to make a decisive contribution to its ambition of reducing net greenhouse gas emissions by at least 55% by 2030 and ultimately becoming climate-neutral by 2050 [1].

The research on the extension of renewable plants also includes a considerable investment in the exploitation of geothermal resources of the various EU member states.

Thanks to the development of new systems for the energy production, district heating, and heat pumps, the exploitation of the geothermal reservoirs is predicted to increase, thus contributing to the reduction in fossil fuels use in energy applications.

With regard to geothermal plants for electricity production, three types of geothermal power plants operate in Europe: conventional (flash and dry steam), binary, and Enhanced Geothermal Systems (EGSs) [2]. The first ones are the most common, although considering the ongoing development, the rise in deployment of the binary and EGS plants is expected, as shown in Figure 1 (based on data from [3,4]).

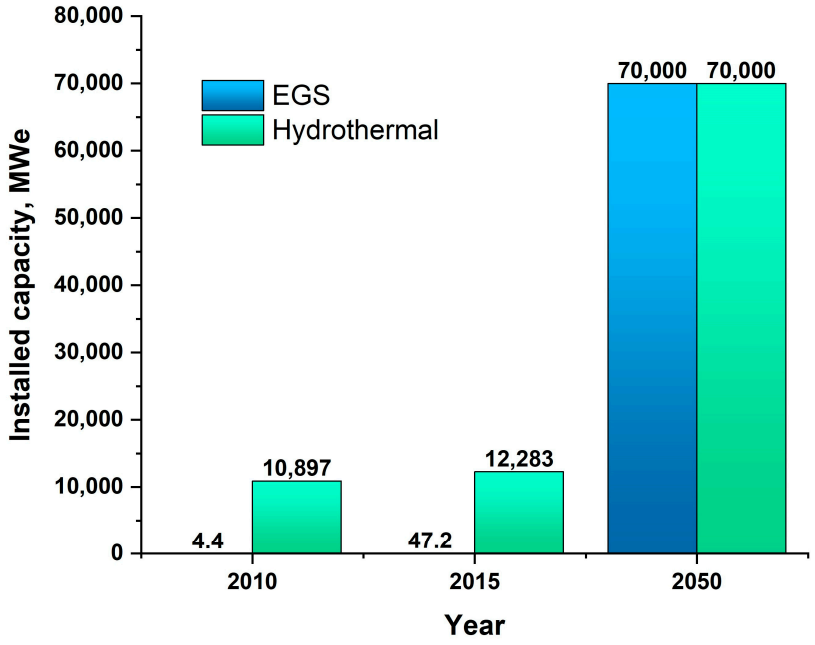

Figure 1. Current state of global installed geothermal capacity.

It is presumed that advancing research, growth, and development in the field of geological formation exploration, drilling, as well as stimulation will continuously be adjusted from the oil and gas sector. Despite the visible progress in enhanced geothermal systems, the EGS technologies are still not mature enough to be commercially competitive with other expanding renewable energy sources such as solar and wind. Operating demonstration EGS plants and their performance would possibly contribute to a significant decrease in drilling costs, which represents the major share in EGS installation cost. Nevertheless, growing attention drawn by developing EGS deployment, especially spotted in countries such as the USA, Great Britain, Germany, China, Iceland and The Netherlands, should be transferred to actions and support from the government and other associated entities in order to provide further technology growth [5].

One of the parameters used to assess the potential power plant is Technology Readiness Level (TRL), which describes the maturity of a given technology. In the case of the enhanced geothermal system, this term includes also the readiness of fracturing, drilling, and energy carrier utilization. Due to issues related to geothermal reservoir establishment, stimulation requirements, interactions between working fluid and rock structure, as well as high costs, the technology readiness remains low. Taking into account the sCO_2 cycles TRL, which is also low (around 4–5), and the fact that the sCO_2-EGS concept is younger than the more developed water-based geothermal systems, the overall sCO_2-EGS technology readiness level may be estimated as 4 in a technology-specific scale, which corresponds to an early stage of development [6–8].

The main goal of this paper is to provide an economic and energy performance assessment of supercritical carbon dioxide enhanced geothermal systems for power generation in order to compare their applicability in a practical point of view. This type of analysis allows for defining the strengths of the various types of Enhanced Geothermal Systems fed by supercritical carbon dioxide (sCO_2-EGS) power plants from both a productivity and

investment perspective, leading to the achievement of a trade-off between the needs and resources in which the system will be installed.

The following paragraphs in this paper give a broader view of the enhanced geothermal systems including a literature review and EGS assessments regarding the energetic performance of different EGS configurations as well as economic evaluation.

1.1. EGS Description

The idea of Enhanced Geothermal Systems (EGSs) is based on the concept of Hot Dry Rock (HDR) first developed in Los Alamos National Laboratory in the USA. HDR is underground bedrock that mainly consists of intact granite or other crystalline basement rock and is characterized by low permeability, low porosity, but significant geothermal potential [9]. The block of hot rock creates a tank located about 5 km below the Earth's surface, whose hydraulic performance has to be artificially increased to enable the heat extraction. Enhancing the flow rate of a working fluid through such tight formations may be achieved with various approaches that have been developed. These methods refer to hydraulic fracturing, chemical stimulation, as well as thermally induced fracturing [10]. The fractures complexity proceeds mainly from their geometry, which is related to different factors including in situ stress conditions, fracturing fluid, and fractures topologies, as well as wellbore direction [11]. The utilization of this accumulated geothermal energy allows for generating electricity on the ground via working fluid, which circulates and collects the heat (Figure 2).

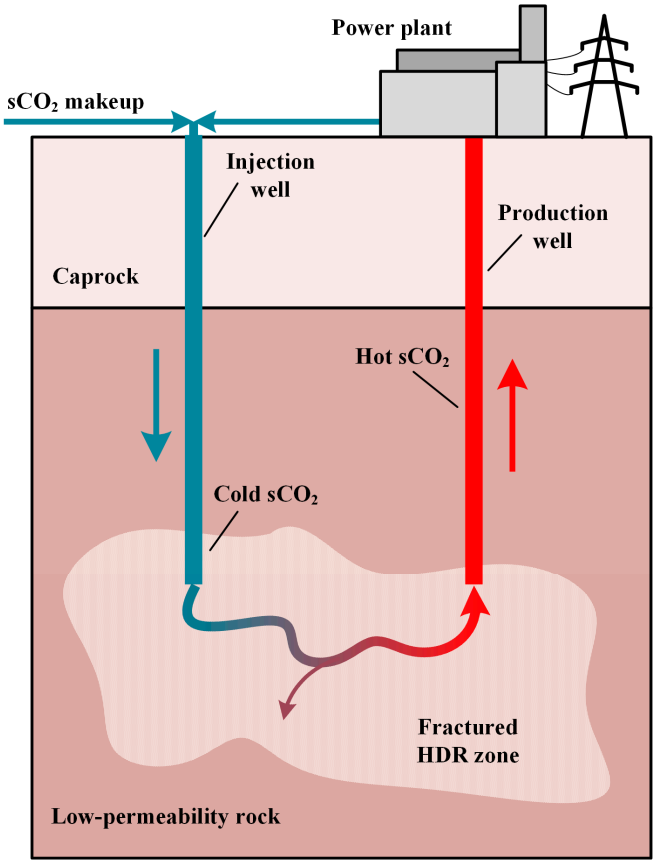

Figure 2. EGS working principle scheme.

The concept is to use hydraulic fracturing to form an artificial geothermal reservoir by creating fractures deep underground. Applied fracturing technologies are widely used in the oil and gas industry, but in EGS systems, they mostly center on shear stimulation of pre-existing natural fractures or are adjusted to create new fractures in geothermal fields. Before EGS development, heat extraction from geothermal resources was possible only

from fractures naturally found in hydrothermal reservoirs with appropriate permeability. Due to hydraulic stimulation, the fractures connect and, thus, the contact area is expanded, resulting in higher energy exchange efficiency [9]. By injecting fluid into the reservoir, the heat is extracted and the hot fluid is brought to the surface to generate electricity or heat. Unlike hydrothermal, EGSs may be feasible anywhere in the world, depending on the economic limits of drill depth and the source temperature available. The choice of the working fluid used to extract the heat from the artificial well depends on the energy availability of the well itself (temperature) and on the thermodynamic properties of the fluid [12].

The first step to set-up an EGS plant is to locate a suitable reservoir with high rock temperature. The site depends on an area with hot, dry rock not on the water accumulated in hydrogeothermal reservoirs as it is conducted in conventional geothermal systems. Then, the wells are drilled and the bedrock is stimulated by hydraulic fracturing to generate a stable network of open, connected fractures that will carry the flow of injected working fluid. Afterward, the fluid circulates through the permeable pathways in the fractured zone collecting the heat and is subsequently extracted by the production well. On the surface, the heat from the fluid is used to produce electricity or electricity and heat in combined systems. EGSs work in a closed loop; thus, the working fluid is headed to the injection well to be reheated. The plant consists of facilities located above and under the ground [13].

Therefore, the most common working fluids used in these power plant types are water, ORC (Organic Rankine Cycle) fluid, and CO_2. The possibility of using different working fluids and the chance of matching it to an ORC make EGS technology an important method of exploitation of geothermal sources, and what also characterizes such a system is the fact that no water is wasted and no gas is released during the HDR utilization [14].

1.2. Comparison of CO_2 and Water

Working fluid in enhanced geothermal systems may be defined as a mixture containing dominant fluid and additives that is applied to create a network of connected fractures. In addition to that, the desired working fluid should be marked by being environmentally friendly with no formation damage, easily available, and feasible, as well as capable of losses control, carrying specific proppants in the formation, and generating a desired net pressure [9]. In a classical EGS, water is applied as a working fluid, although there are some promising gas fluids that may become more advantageous. Due to its thermodynamic properties and environmental benefits, CO_2 as a working fluid becomes an attractive option [2]. Table 1 presents the differences between water and CO_2 as a working fluid in enhanced geothermal systems.

Table 1. Comparison of CO_2 and H_2O as a working fluid in EGS [12].

Fluid Properties	CO_2	H_2O
Chemical	Not an ionic dissolution product. No mineral dissolution/ precipitation problems	An ionic dissolution product. Effective solvent for rock minerals, may cause serious problems of mineral dissolution/precipitation
Fluid circulation	Higher compressibility and expansivity. Greater mass flow rates	Lower compressibility. Moderate expansivity. Lower mass flow rates
Ease of flow in the geothermal reservoir	Lower viscosity and density	Higher viscosity and density
Heat transmission	Lower specific heat capacity	Higher specific heat capacity
Fluid losses	Favorable potential for geological sequestration of CO_2	A drawback for commercial operation

The idea of a CO_2-EGS was proposed at first by Brown in 2000 [15]. It was suggested that CO_2 may be more beneficial than water in such plants. This system has an advantage of possible permanent CO_2 sequestration through fluid losses at great depths during its

operations, which seems crucial in case of the need to reduce carbon emissions. CO_2 is less effective as a solvent for most rock minerals and its larger compressibility and expansiveness reflect the strong natural buoyance force that yields larger self-propelled flow velocities and less power consumption needed for the fluid circulation system. Furthermore, CO_2 is seen as a more favorable solution due to its lower viscosity, which results in higher mobility and better transport properties, and partly compensates the lower-than-water mass heat capacity by greater flows.

The advantage of EGS plants is the possibility to utilize part of the CO_2 captured from fossil-fired power plants and other emitters, preventing emissions to the atmosphere. Despite that, these systems have to face some challenges.

1.3. The Application of sCO_2 Cycles

According to the international targets on the reduction in carbon dioxide production, new low-emission power plants, more efficient renewable energy systems, and new CO_2 capture systems will be case studies in the coming years.

The sCO_2 cycle represents one of the most important ways to improve the cost-effectiveness of carbon capture and storage (CCS) technologies using CO_2 captured before its permanent geological storage [8]. Thermal-power cycles operating with supercritical carbon dioxide could have a significant role in future power generation systems with applications including fossil fuel, nuclear power, concentrated-solar power, and waste-heat recovery.

The use of sCO_2 as both reservoir fracturing fluid and working fluid has been initially proposed by Brown in a study [15] mainly focused on the geological perspective (the sCO_2 not being a good solvent results in a significant reduction in the scaling problems that makes sH_2O reservoir development unfeasible). The following studies [16,17] have shown that the sCO_2 is also capable of generating a significant thermosyphon effect due to the density gradient between the injection and production wells. This allows for the direct expansion of the working fluid in a turbine, greatly simplifying the surface plant physical footprint and improving the operational flexibility, which could result in lower levelized costs of electricity compared to existing technologies [18]. On the other hand, water-based systems are usually more appealing for heat-driven application (DH systems, Closed Binary Cycles) due to the higher specific heat of H_2O compared with sCO_2.

1.4. Working Fluids in ORC-EGS

The ORC working fluid selection is critical for the system performances, and multiple studies [19,20] have analyzed different aspects of fluid selections. Many technical, economic, and environmental aspects, often conflicting with each other, must be considered when selecting the working fluid, and the detailed guideline has been proposed by Quoilin et al. [21] and can help in the selection process.

In practice, however, only a few fluids are used by industries while developing a geothermal binary plant, for economic, environmental, and industry standardization reasons. The most common fluids are:

- Alkane (n-pentane, i-butane) mainly used by ORMAT in their binary plants [21,22];
- OMTS (Organosilicon compounds), mainly used by Turboden [21];
- Refrigerant Gasses (R-134a, R245fa, R1233zd [23]);

I-butane has been used in our model because it is an industry standard and in view of the expected geothermal fluid temperature condition.

2. Materials and Methods

2.1. Case Study Selection

Depending on the heat demand type as well as possibility to obtain temperatures and pressures of the supercritical CO_2 at the outlet of the production well, three types of energy generation scenarios could be investigated:

- Power generation only;
- Heat generation only;
- Combined heat and power generation.

Due to the reduced thermal capacity of the geothermal region with which the modeling of the power plants was implemented, electricity generation became the primary goal. However, it was decided to introduce a specific power plant with an installation for a district heating system (DHS) in order to evaluate the exploitation of the resource in a combined power plant.

Four groups of cycles can be distinguished:

	Case	Abbreviation	Comment
1.	Direct supercritical CO_2 cycle	D_sCO_2	Figure 3a
2.	Indirect sCO_2 cycle with ORC (binary cycle)	I_sCO_2_ORC	Figure 3b
3.	Direct supercritical CO_2 cycle with cogeneration;	D_sCO_2_DHS$_A$	DHS located between turbine stages, Figure 4a
		D_sCO_2_DHS$_B$	DHS located after the production well, Figure 4b
4.	Direct sCO_2 cycle combined with ORC	D_sCO_2_ORC$_A$	Recovery heat exchanger located before the injection well, Figure 5a
		D_sCO_2_ORC$_B$	Recovery heat exchanger located after the production well, Figure 5b

The Direct sCO_2 cycle, presented in Figure 3a, represents the simplest cycle for the exploitation of the geothermal resource. This power plant foresees a direct expansion in the dedicated turbine of the sCO_2 coming from the geothermal well. After that, the sCO_2 is cooled before the injection well, and the heat released to the cooling fluid is not recovered. Due to partial CO_2 sequestration (sequestration rate around 5%), an additional CO_2 stream supplies the cycle. In the second case (Figure 3b), which shows an indirect sCO_2 cycle with the ORC, the electric power is generated only by the expansion in the turbine in the ORC. The sCO_2 in the geothermal well works in a closed loop and is used as a hot source to feed the Organic Rankine Cycle via a dedicated heat exchanger. Heat extracted by sCO_2 in the reservoir is transferred to the ORC working fluid, which circulates in the cycle containing basic elements: turbine with generator, condenser, and pump.

The next two implemented models represent two solutions where the goal is to maximize the recovery of energy that is lost from the sCO_2 cycle by cogeneration application. These two configurations are based on the already presented, basic direct sCO_2 cycle, which was extended by adding an extra heat exchanger for heat transfer to circulating water in the DHS. Both variants are presented in Figure 4 and the distinction between them relies on the location of the applied heat exchanger.

A direct supercritical CO_2 cycle with cogeneration combines electricity production with heat generation for the district heating system. In this work, two different arrangements were analyzed:

- DHS between turbine stages with lower source temperature (Figure 4a);
- DHS after outlet production well with higher source temperature (Figure 4b).

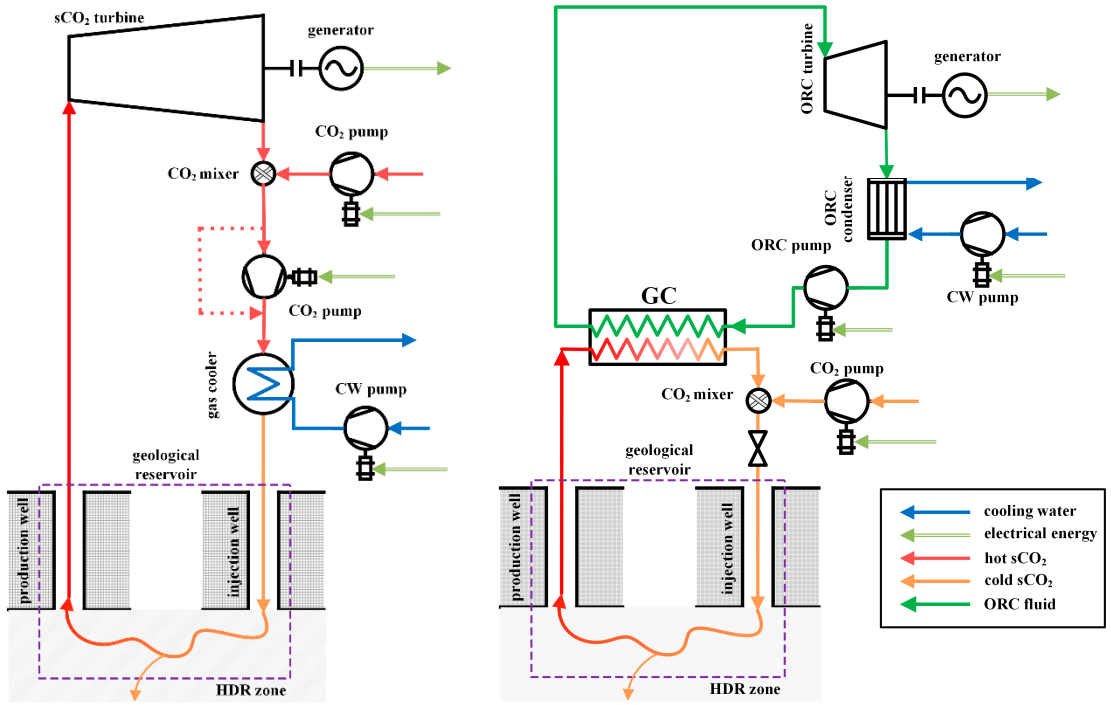

(**a**) (**b**)

Figure 3. Simplified schematic diagrams of (**a**) direct sCO_2 cycle and (**b**) indirect sCO_2 cycle with ORC.

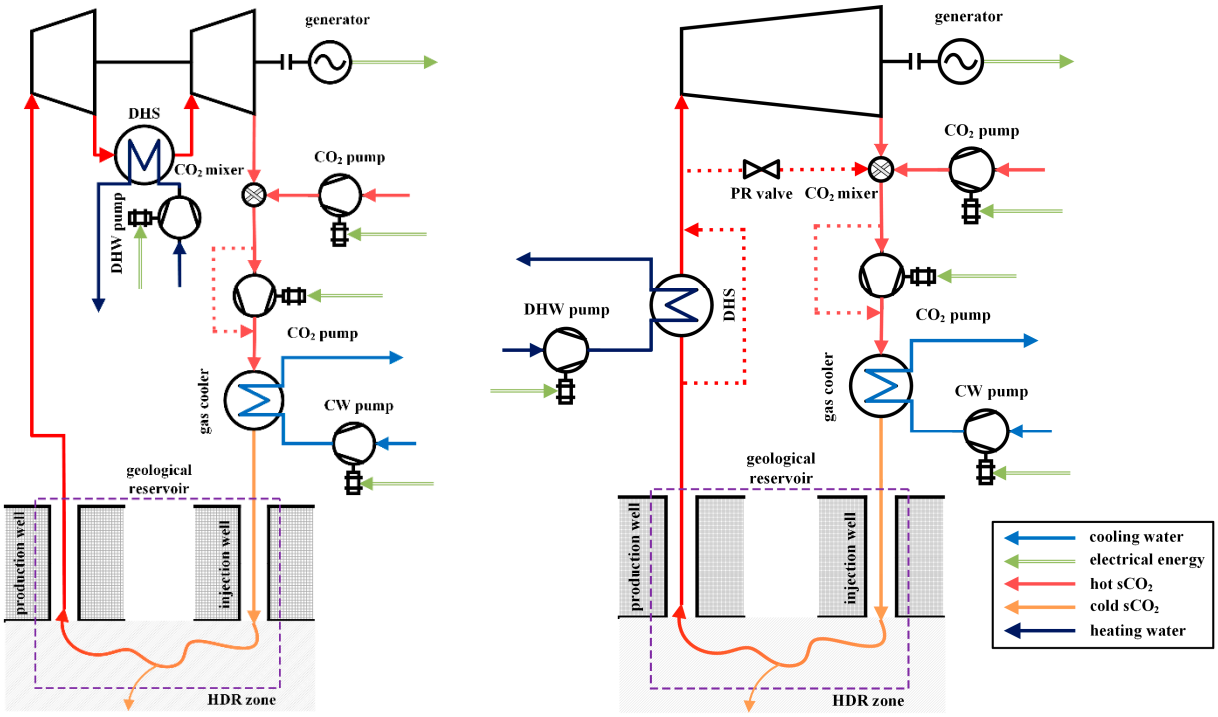

(**a**) (**b**)

Figure 4. Simplified schematic diagrams of direct sCO_2 cycle with cogeneration; (**a**) DHS between turbine stages; (**b**) DHS after the production well.

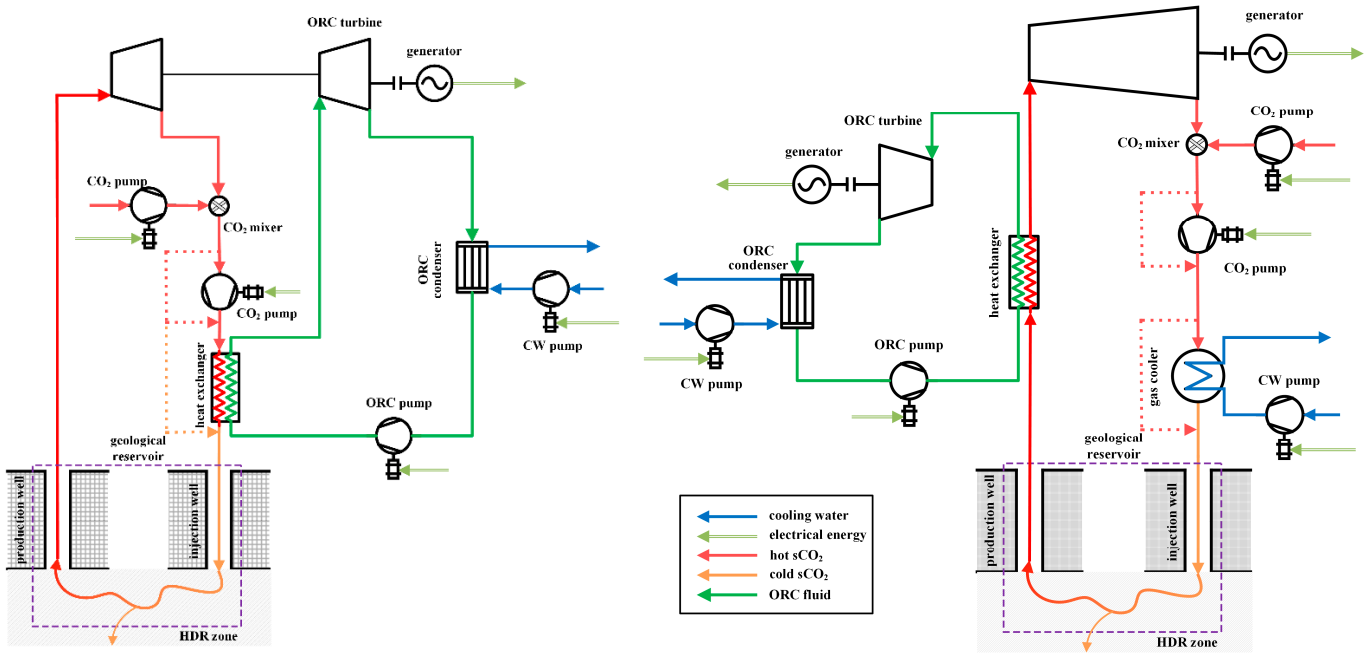

Figure 5. Simplified schematic diagrams of direct sCO_2 cycle with ORC: (**a**) recovery before the injection well; (**b**) recovery after the production well.

Looking for the best solution for recovering the heat released in the direct sCO_2 cycle, in order to maximize electricity production and cycle efficiency, a combined power plant with a direct sCO_2 cycle and ORC was modeled. Those configurations match the direct sCO_2 expansion in the turbine as well as the heat transfer through the heat exchanger to the Organic Rankine Cycle. According to this, two different systems of combined power plant were proposed:

- Recovery heat exchanger before inlet of the injection well (Figure 5a);
- Recovery heat exchanger after outlet of the production well (Figure 5b).

2.2. Analytical Model Description

This subsection presents the process of mathematical modeling of the sCO_2 cycles, which are intended to be applied for utilization of the heat extracted from the geothermal reservoir. On the basis of the set of configurations described in the previous section, mathematical models of the direct sCO_2 Brayton cycles for electricity production or cogeneration were developed. For this purpose, the Engineer Equations Solver (EES) software was used. This tool was designed for calculating energy balances and simulating processes.

Engineer Equations Solver is a software used for solving engineering problems based on the resolution of a system with n equations and n unknowns.

For each plant configuration, a numerical model was implemented using EES with the aim of calculating the thermodynamic points of the cycle, and the mass and energy balances for each component of the plant. Moreover, through the tools of the software (parametric analysis), it was possible to determine the performance parameters of each configuration to vary the parameters of the geothermal reservoir. A model of the reservoir itself was prepared using work [24].

It is worth pointing out that all configurations have common basic components to ensure the same exploitation of the resource. Having similar configurations and the same components allowed for making a comparison between the various solutions, in addition to achieving comparable results.

As shown in the previous section, four different cases of the sCO_2 cycles were proposed:

Direct sCO_2 cycle

Due to the CO_2 thermosiphon effect, no additional CO_2 compressor is necessary in all configurations analyzed in this work. After the sCO_2 passes through the turbine, mass flow losses are replenished in the mixer through a sCO_2 feed pipeline. Then, it is cooled down in the gas cooler and flows to the injection well. The turbine outlet pressure is defined as the sum of the required pressure at the inlet of the injection well and the pressure loss in the gas cooler.

Indirect sCO_2 cycle with ORC (binary cycle)

The sCO_2 is not directed to expansion in the turbine. The sCO_2 from the production well goes through a heat exchanger, where the heat is transferred to the working fluid in the ORC and then sCO_2 is cooled using a laminar valve, in order to obtain the required injection well's pressure and temperature. The ORC working fluid at vapor-saturated conditions passes through the turbine to be consequently cooled down until it reaches liquid-saturated conditions.

Direct supercritical CO_2 cycle with cogeneration

Heat and power generation are the main products in such units. Heat is recovered with a DHS before the turbine inlet or with a DHS located between two stages of the turbine. Power generation is obtained via sCO_2 expansion in the turbine or as with the other case with the passage of the sCO_2 in the two turbine stages. After the expansion and crossing of the mixer, the carbon dioxide is cooled down but the heat released is not recovered (waste heat).

Combined direct sCO_2 with Organic Rankine Cycle

Direct expansion in the sCO_2 turbine and ORC allows electricity production to be achieved. It is characterized by matching the direct sCO_2 cycle and ORC. The sCO_2 cycle works exactly as described in previous systems, but the combination with the ORC was proposed in two different ways. The first solution refers to feeding the ORC through the heat recovery released by the heat exchanger before the injection well, and the second case involves the use of a heat exchanger located after the production well outlet. The operation of the ORC is the same as that described in the binary configuration.

The working fluid used in the Organic Rankine Cycle is isobutane. This fluid was chosen due to its considerable use in the ORC and the fact that natural gas derivatives are generally cheaper. On the contrary, the use of chemical refrigerants is not recommended, as they are considered to be contaminative (e.g., R134a) or very expensive (e.g., R1233zd(e)).

2.3. Process Synthesis and Design

- Geothermal Well

For each power plant, the same geothermal well was used as an energy source for the thermodynamic cycle. The geothermal well model was implemented by defining the temperature and flow rate of CO_2 in the injection well; these two parameters represent the independent variables from which it was possible to calculate the pressure, flow, and temperature values of the production well by the use of the EES interpolation function.

According to the model, ranges of temperature and mass flow for the CO_2 injection well were set as:

$$20\ [\mathrm{kg/s}]\ \leq \dot{m}_{inj} \leq 200\ [\mathrm{kg/s}] \quad (1)$$

$$35\ [^{\circ}\mathrm{C}] \leq T_{inj} \leq 55\ [^{\circ}\mathrm{C}] \quad (2)$$

All configurations were simulated by changing the parameters of $\dot{m}_{inj}$ and T_{inj} within the fixed ranges. Therefore, it was possible to identify the parameters (mass flow, pressure, and temperature) of the geothermal wells corresponding to the maximum production of electricity.

- Pipeline

In all models implemented, the supercritical CO_2 cycle was fed by carbon dioxide from pipelines to replace the mass flow losses. The mixer after the turbine outlet allowed for matching the sCO_2 feed system with the main stream into the supercritical cycle. The

origin of the mass flow losses is due to the transition of CO_2 in the geothermal well: the interaction of the carbon dioxide with chemical substances present in the subsoil leads to the oxidation of part of the CO_2, causing a reduction in the effective outgoing mass flow from the production well.

- Main compressor

All sCO_2 cycles in each configuration include a compressor (main compressor) located between the mixer and the condenser/heat exchanger. This compressor goes into operation for maintaining the required pressure at the injection well inlet in the case of excessive pressure drop due to the components of the power plant. In Table 2, a summary of the main assumptions for system components is presented.

Table 2. Summary of modeling assumptions.

Parameter	Value
Isentropic Efficiency	
sCO_2 Turbine	90%
sCO_2 Compressor pipeline	94%
Relative pressure losses in heat exchangers	0.5–1 bar
Minimum temperature difference for heat exchangers	10–25 °C
Isentropic Efficiency	
ORC Turbine	78%
ORC Pump	70%
Mechanical efficiency	
Turbine-generator	98%
Compressors motors	98%
Pump motors	98%
Electrical efficiency of generator	96%
Water cooling systems	
Pressure cooling	2 bar
Temperature water inlet	12 °C
ΔT water	10 °C

Due to different temperatures in units with cogeneration, it was assumed that in the first case, D_sCO_2_DHS_A, where the heat exchanger for the district heating system is located between the turbines, the temperatures of water at the cold and hot side will be, respectively, 35/60 °C, which is suitable for the low-temperature DHS (LTDHS). The low-temperature system usually refers to temperatures between 50 and 60 °C and is rated as modern 4th-generation district heating [25]. In the second case (D_sCO_2_DHS_B) where the DHS heat exchanger is located after the production well, the water temperatures were assumed to be 50/80 °C, which represents typical values for the Polish district heating system (3rd generation). Different water temperature values will not have an impact on further economic evaluation, because of the exergetic allocation method used for calculations.

2.4. Economic Assessment

For the purpose of economic comparison of the analyzed EGS cases, the total system capital expenditure (*CAPEX*) was evaluated with the following formula:

$$CAPEX = C_{well} + \sum C_{EGS} + \sum C_{i,EQP} + C_{direct,EQP} + C_{indirect,EQP} \quad (3)$$

$$C_{well} = C_{well,unit} \cdot n_{well} \cdot d \quad (4)$$

CAPEX consists of the costs of drilling the wells C_{well}, which depends on the unit cost of drilling one well $C_{well,unit}$; the number of wells n_{well}; the well depth d; costs associated

with one well-doublet development (including hydraulic fracturing of the EGS zone), C_{EGS}; the cost of installed equipment C_{EQP}; as well as the cost of secondary equipment (pipes, valves, civil engineering, instrumentation, and control equipment), including the cost of transportation, the land cost, civil and structure cost $C_{direct,EQP}$, and indirect cost, which denotes engineering, supervision, and plant start-up costs $C_{indirect,EQP}$.

The calculations were performed using the methodology presented in [26]. Presented costs were updated to EUR2021 from their origin years due to EUR/USD exchange rates.

Equipment cost was obtained from the following equations applied for turbomachinery and heat exchangers separately:

For turbomachinery:

$$C_{i,EQP} = a \cdot (|W|)^b \cdot f_p \cdot f_t \tag{5}$$

For heat exchangers:

$$C_{i,EQP} = a \cdot (|UA|)^b \cdot f_p \cdot f_t \tag{6}$$

where factors f_p, f_t refer to maximum pressure and temperature, respectively, for sCO_2 installed components. The following correlations allow the influence of high pressure and temperature on the equipment materials to be taken into consideration.

$$\begin{cases} f_p = 1 \ \ if \ p_{max} < 10 \text{ MPa} \\ f_p = 0.8 + 0.2 \cdot p_{max} \ \ if \ \ p_{max} \geq 10 \text{ MPa} \end{cases} \tag{7}$$

$$\begin{cases} f_T = 1 \ \ if \ T_{max} < 400 \text{ °C} \\ f_T = 5.32 - 0.0238 \cdot T_{max} + 0.00003 \cdot {T_{max}}^2 \ \ if \ \ T_{max} \geq 400 \text{ °C} \end{cases} \tag{8}$$

The functions Equations (5) and (6) include W, which relates to the power of machinery (turbine, compressor, pump, and generator) (MW); UA, which denotes the multiplication of the overall heat transfer coefficient U and heat transfer area A (kW/K); 'a' and 'b' parameters, which depend on the component.

Further financial assumptions are presented in Table 3.

Table 3. Summary of financial assumptions.

Parameter	Value
Cost year basis	2021
Base currency	EUR
Project lifetime, n	25
Annual plant availability, τ_{an}	7008 h
Discount rate, r	8%
Annual operating expenditures, $OPEX$	3% of $CAPEX$
Unit cost of drilling well, $C_{well,unit}$	1404 EUR/m
Cost associated with EGS system, C_{EGS}	1,460,415 EUR
Turbomachinery [26] Equation (5)	
sCO_2 turbine	a = 168 840; b = 0.8
sCO_2 compressor	a = 134 400; b = 0.8
Heat exchangers [26] Equation (6)	
chiller	a = 168; b = 1
recuperator	a = 420; b = 1
Direct equipment costs, $C_{direct,EQP}$ [26]:	
piping	3% of $\sum C_{i,EQP}$
instrumental and control	5% of $\sum C_{i,EQP}$
land	3% of $\sum C_{i,EQP}$
civil and transportation	15% of $\sum C_{i,EQP}$
Indirect equipment cost, $C_{indirect,EQP}$ [26]	8% of $(\sum C_{i,EQP} + C_{direct,EQP})$

All other necessary assumptions regarding equipment costs in sCO_2 cycles and Organic Rankine Cycles were taken from [27,28].

The economic evaluation also includes the performance of Levelized Cost of Electricity for all analyzed cases and Levelized Cost of Heat for combined cycles. The levelized costs enable the comparison to be made of plants in the case of their system profitability and to relate to the average electricity or heat prices that have to be incurred for energy generation during the unit lifetime. The *LCOE* and *LCOH* were calculated based on the following formulas:

$$LCOE = \frac{\varepsilon_{B,el} \cdot (CAPEX \cdot f_r + \sum_i OPEX_i)}{E_{el}} \quad (9)$$

$$LCOH = \frac{\varepsilon_{B,Q} \cdot (CAPEX \cdot f_r + \sum_i OPEX_i)}{Q} \quad (10)$$

where $OPEX$ refers to operational expenditures; E_{el} is annual electricity generation, Q is annual heat production for the DHS; $\varepsilon_{B,el}$ and $\varepsilon_{B,Q}$ are total system cost multipliers, which enable specific cost allocation to electricity and heat production, respectively, obtained within the exergy allocation methodology [29]; f_r is a discount factor calculated as follows:

$$f_r = \frac{r(1+r)^n}{(1+r)^n - 1} \quad (11)$$

where r is the discount rate and n is years of project lifetime.

3. Results

3.1. Energy Assessment

The obtained results show the potentialities of the different simulated power plants. As presented, the discussed results are based on the developed mathematical models and conducted simulations. Due to the lack of experimental data from pilot or demonstration plants, it is impossible to validate the results of the whole CO_2-EGS analyzed, but the performance of the Bryton CO_2 cycles is within the range of results from similar studies.

In the first analysis, the net power is the main parameter with which the plants were compared. However, an exclusively developed comparison of net output power would be limiting. Each plant must be contextualized to the field of application and the necessary resources to obtain the plant power. On this basis, the analysis of the results obtained in this paper provides a comparison of all the models, with the aim of determining the best design solutions according to the varying application conditions. In Figure 6, the net power of the analyzed systems is presented.

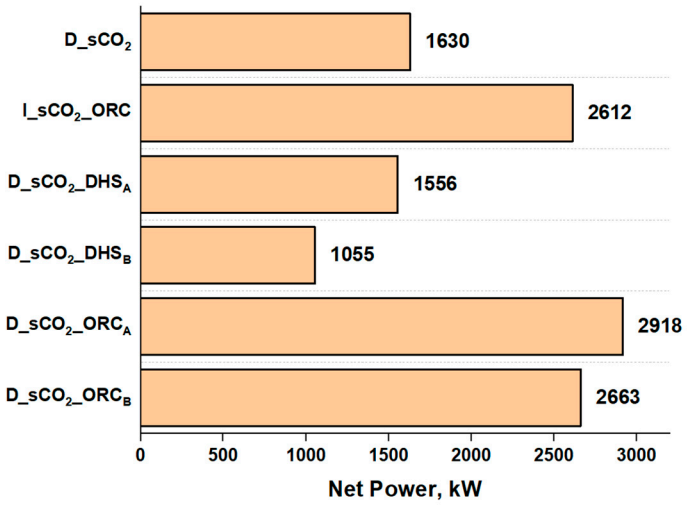

Figure 6. Net power of the analyzed configurations.

Targeting the maximum available power generation, the hybrid power plants' sCO_2 + ORC turn out to have the highest value of power generation. Furthermore, placing the heat

exchanger at the inlet of the injection well leads to more power. As expected, the direct supercritical CO_2 cycle with cogeneration returns a lower power (high percentage of heat production).

The direct sCO_2 cycle generates a reduced power compared to hybrid cases, but the generated power ratio and design complexity makes it a very advantageous solution.

Simulations show that plants with a greater potential for the production of electricity have a hybrid cycle sCO_2 + ORC and binary cycle. Therefore, the comparison of these two models in terms of power production was conducted.

From the plots in Figure 7, it can be observed that in the binary model, the power is directly proportional to the flow of sCO_2: increasing the flow yields a higher power as the supercritical cycle is detached from the power cycle (hot source).

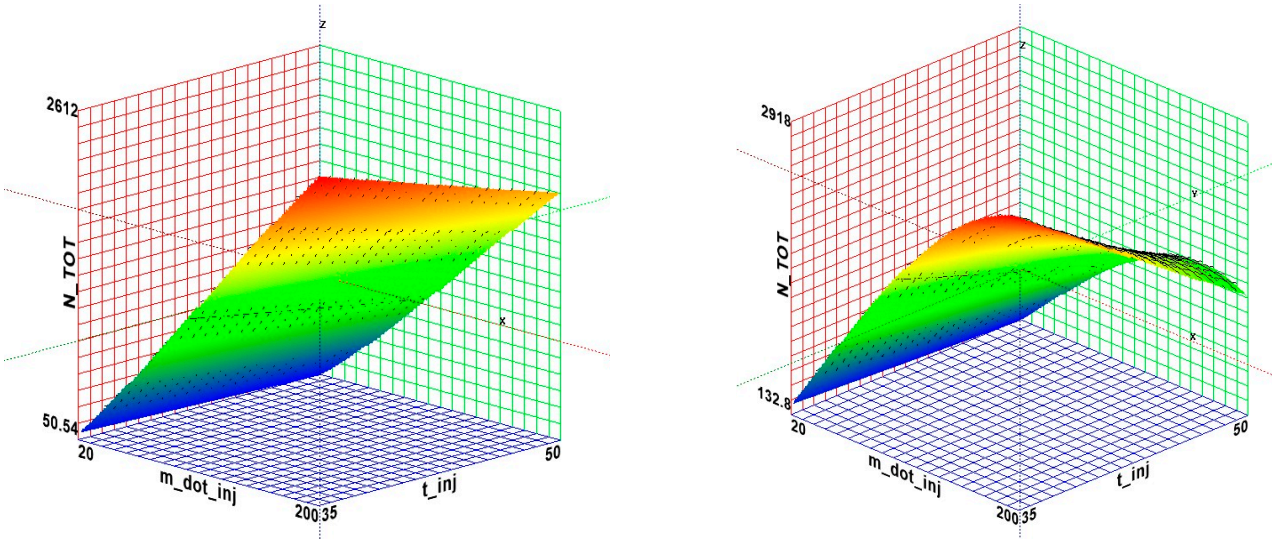

(**a**) (**b**)

Figure 7. Three-dimensional plots for (**a**) binary cycle and (**b**) direct sCO_2 cycle with ORC (heat recovery before injection well).

On the other hand, in the hybrid models, the power generated has a maximum point corresponding to a certain mass flow of sCO_2. Further increasing the mass flow is conducive to decreasing the power, as the total value of the net power is obtained from the sum of the net powers generated by the cycle ORC and sCO_2. The inflection point can be explained by tracing the separate course of the two power inputs corresponding to the two cycles ORC and sCO_2. In the plot in Figure 8, it can be noticed that while increasing the mass flow, the power generated by the sCO_2 cycle and ORC has the opposite trend: at high flow rates, the contribution of the power ORC system is preponderant in comparison with the power of the sCO_2 cycle; on the contrary, for lower mass flow rates, the supercritical cycle generates a higher power.

For low sCO_2 mass flow, power generation from the ORC is negligible compared to sCO_2. Due to low mass flow and lower temperature output from the production well, the heat recovered from the ORC is limited. Therefore, the use of a sCO_2 direct expansion cycle without a parallel ORC is the best solution for power generation (improved plant power and investment costs ratio).

For high sCO_2 mass flow, the power generated in the sCO_2 cycle decreases unlike the trend of ORC net power. The use of the sCO_2 as well as a hot source in a binary cycle is the best solution for power generation in this configuration as the binary cycle has the maximum net power generated for the highest mass flow available.

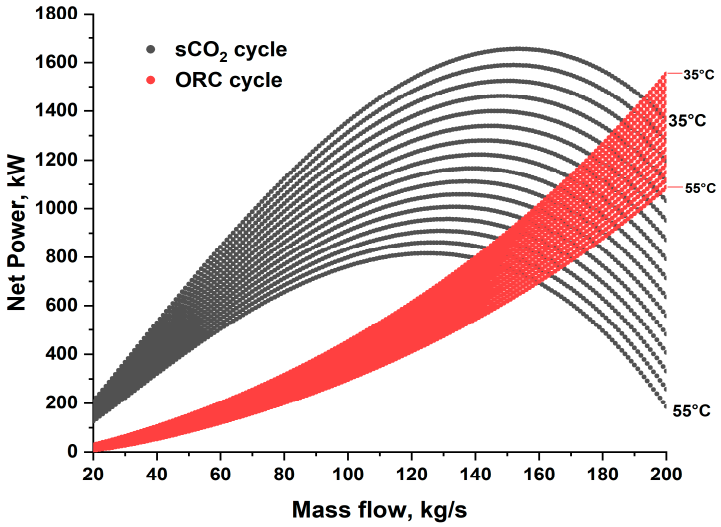

Figure 8. The comparison of sCO_2 and ORC in the case of net power with variable mass flow rates and injection temperatures between 35 and 55 °C.

Not only is the power generated important, but also the conditions under which maximum electricity production is achieved. In this regard, the plot in Figure 9 allows the definition of the value of the well's parameters that identify the peak of the energy production at the well inlet temperature of 35 °C (temperature corresponding to maximum power values).

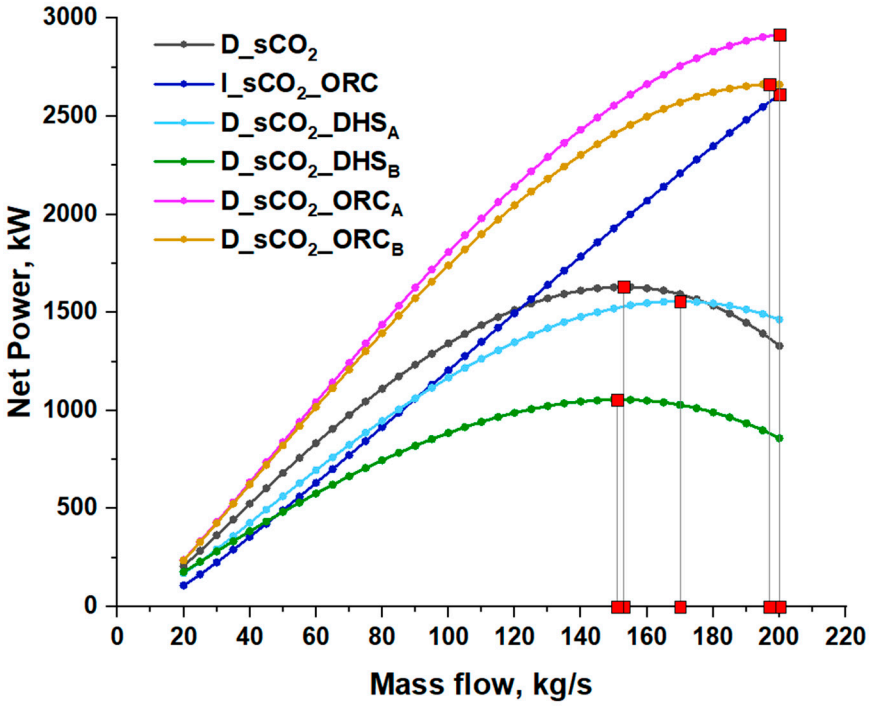

Figure 9. The change in net power with variable mass flow rates for analyzed configurations and peak points (marked as red squares) obtained for maximum power generated in each system.

For the same injection temperature, the configurations may be compared in the case of unitary net power output, which is the obtained net power divided by the mass flow rate (Figure 10). This gives a different perspective on the dependence between generated power and sCO_2 flow rate; nevertheless, the conducted analysis shows that the highest power was reached in direct cycles with the ORC.

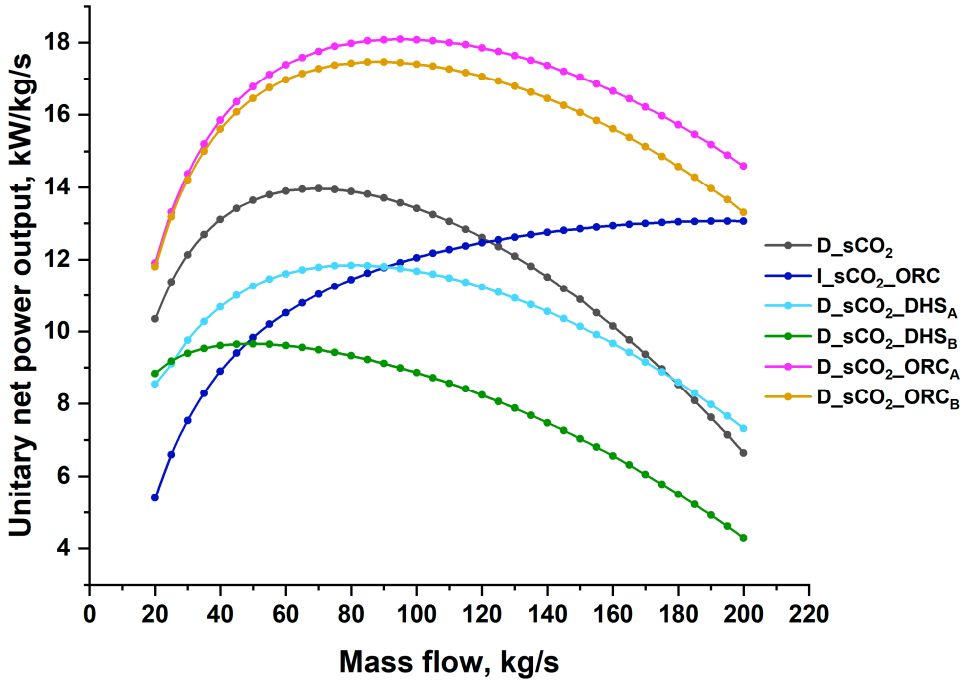

Figure 10. The change in unitary net power with variable mass flow rates for analyzed cases.

Analyzing the power plants with cogeneration, inevitably, the power generated is not comparable to other plants, but it is possible to compare the two analyzed solutions in which the location of the DHS is different (Figure 11).

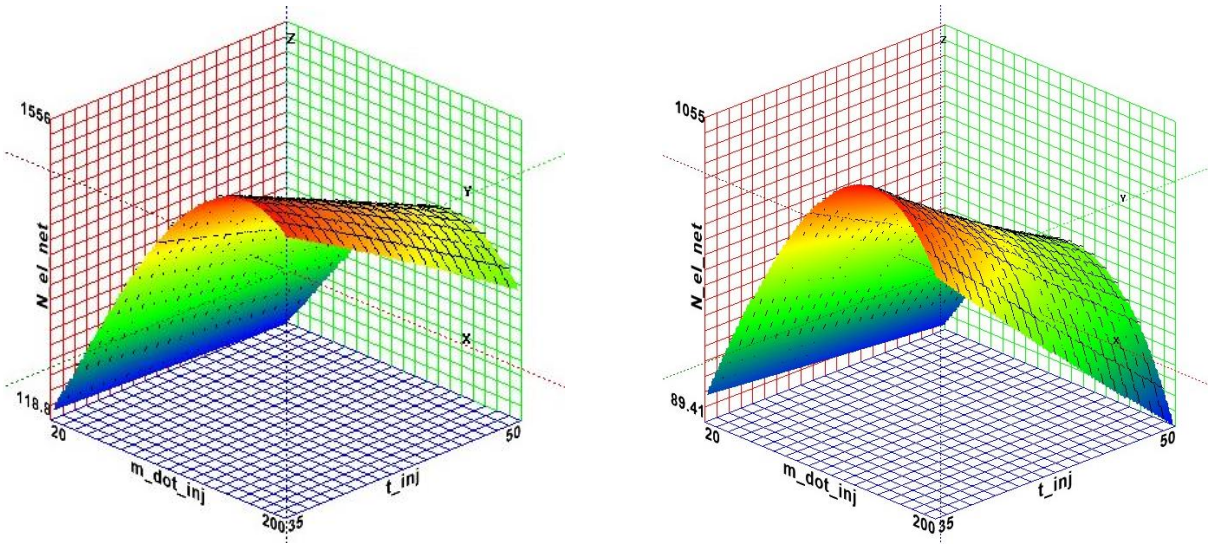

(**a**) (**b**)

Figure 11. Three-dimensional plots for sCO_2 with DHS located (**a**) between turbine stages and (**b**) after the production well.

The DHS located at the outlet of the production well and before the sCO_2 turbine inlet promotes the production and recovery of heat because the enthalpy of the working fluid is high. This, however, involves a reduction in the ΔH in the turbine unfavorable for the production of electricity. Instead, placing the DHS between two turbine stages allows a higher output power to be obtained but with a lower enthalpy heat source for heat generation.

3.2. Economic Evaluation

Figure 12 shows the *CAPEX* distribution in the analyzed cases. In all six systems, the cost of drilling was the same (the same depth and number of wells) and it represents the biggest share in *CAPEX* of EGS systems up to 80.3% of the total investment cost. In the direct sCO_2 case, this share is highest because of just a few components, which are associated with the lowest equipment cost. The high pressure and temperature values impact the heat exchanger operation, especially in the indirect sCO_2 cycle; thus, in this case, the cost of heat exchangers components is highest.

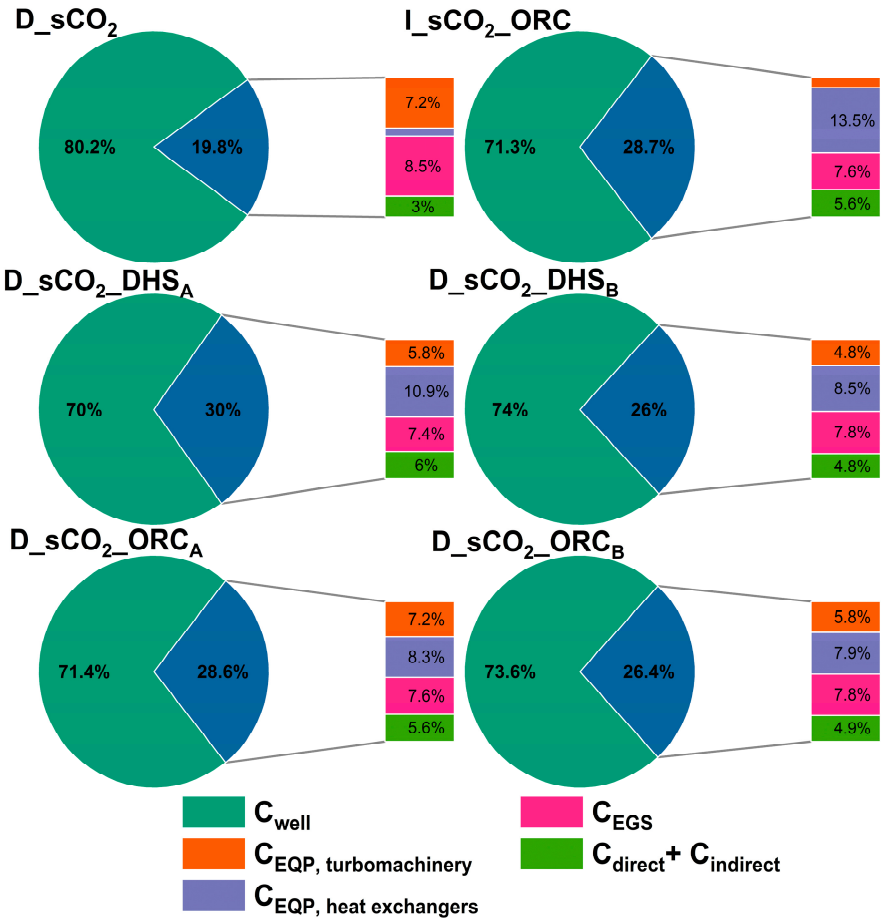

Figure 12. *CAPEX* distribution within the analyzed cases.

A summary of the economic evaluation containing *CAPEX*, *OPEX*, as well as the values of Levelized cost of electricity and heat (for combined cycles) is presented in Table 4. The highest levelized cost was obtained in the binary cycle due to the relatively high capital costs and low electricity production. The *LCOH* was performed for variants with cogeneration, and this parameter is slightly smaller in the case where the DHS heat exchanger is located after the production well; nevertheless, both values are within an acceptable range.

In Figure 13, the correlation between the obtained *LCOE* for each variant with increasing discount rate up to 20% is presented. The graph shows a wider perspective on how the discount factor influences the costs of a project. For all cases, the growth of *LCOE* with the rising values of discount rate is visible; however, as shown in Table 4, the indirect cycle becomes the highest *LCOE*, while direct cycles integrated with the district heating system become the lowest.

Table 4. Summary of Levelized Cost of Electricity and Heat.

Case	*CAPEX* M EUR	*OPEX* M EUR	*LCOE* EUR/MWh	*LCOH* EUR/GJ
D_sCO_2	17.17	0.10	169.13	n/a
I_sCO_2_ORC	19.30	0.17	219.47	n/a
D_sCO_2_DHS_A	19.68	0.18	141.11	2.75
D_sCO_2_DHS_B	18.60	0.14	118.02	3.87
D_sCO_2_ORC_A	19.28	0.17	145.04	n/a
D_sCO_2_ORC_B	18.69	0.15	139.58	n/a

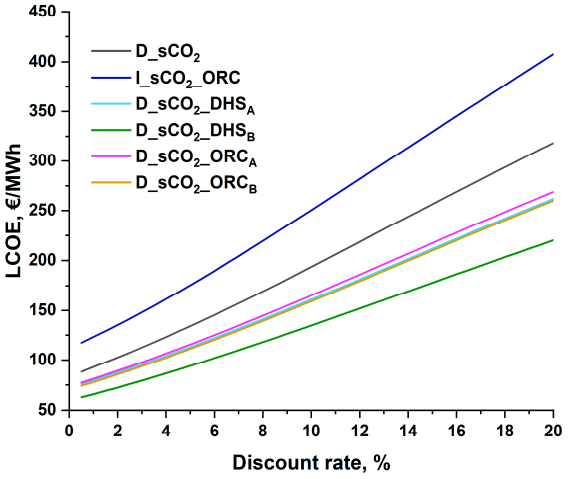

Figure 13. Correlation between *LCOE* and discount rate for analyzed cases.

For the direct sCO_2 cycle combined with the ORC where the recovery heat exchanger is located before the injection well, the change in *LCOE* with the sCO_2 mass flow was performed (Figure 14). With the lowest value of 20 kg/s, the *LCOE* reached almost 900 EUR/MWh; thus, it would be not economically viable to build a unit with such a low mass flow. For mass flows between 100 and 200 kg/s, the obtained *LCOE* has similar values but the net power differs; therefore, it is essential to choose the optimal solution.

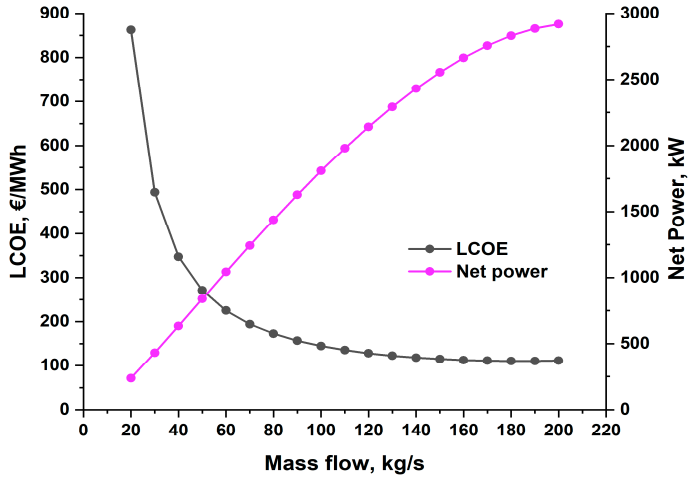

Figure 14. Change in *LCOE* and Net Power with increasing mass flow for case.

4. Discussion

The purpose of the paper was to compare and discuss the energetic and economic performances of enhanced geothermal systems based on sCO_2 cycles.

The results show the strengths of different types of power and heat generating systems built on the geothermal reservoir. Nevertheless, there is a difficulty in identifying the best solution as the choice will depend on the useful effect obtained from the geothermal source.

- Power generation

The use of the combined direct sCO_2 with the ORC allows the power plant efficiency to be optimized by recovering part of the heat released from the sCO_2 cycle to produce additional electricity but with greater design complexities. On the other hand, the binary cycle would allow for high power outputs, but the use of sCO_2 as working fluid would limit the geothermal heat recovery. This favors the use of working fluids that would provide a higher heat recovery than sCO_2 (e.g., water).

- Cogeneration

The performance of the variants analyzed in this paper was evaluated over a wide range of sCO_2 flow rates, temperatures, and pressures. What should be stressed in these units is a beneficial impact on the wellhead pressure difference, which causes a thermosiphon effect and subsequently leads to no requirement of an additional CO_2 compressor before the injection well. However, to study the design feasibility of combined power plants, it is necessary to analyze the technological availability of turbomachinery (compressors and turbines) working with sCO_2 (design constraint).

From the economic perspective, the capital and operational expenditures were highest for the direct sCO_2 cycle with cogeneration where a heat exchanger was added between turbine stages, but similar values were obtained for the indirect cycle and, for this case, the *LCOE* was highest. For all analyzed cases, the *LCOE* varied between 118 and 220 EUR/MWh. For low mass flow rates, the sCO_2-EGSs are not financially justified, because of high costs of electricity as well as low electricity production. Due to recent fluctuations in the energy market and associated variable electricity prices as well as low technology readiness level that influences high capital expenditures, the EGS payback period is not feasible within 25 years of project lifetime and the internal rate of return is lower than the assumed discount rate. These research findings emphasize the need of financial support for further development and deployment of enhanced geothermal systems, especially when we consider the benefit of possible CO_2 partial permanent storage.

Author Contributions: Conceptualization, M.T. and P.G.; methodology, M.T., P.U. and M.S.; software, M.T., P.U. and P.G.; validation, M.T., T.A. and P.U.; formal analysis, L.T. and D.F.; investigation, M.T., P.U., M.S. and P.G.; resources, P.U., M.S. and G.M.; data curation, M.S., L.T. and A.S.; writing—original draft preparation, M.T., P.U., P.G. and M.S.; writing—review and editing, P.G. and M.S.; visualization, M.T. and M.S.; supervision, P.G., L.T. and A.S.; project administration, P.G. and L.T.; funding acquisition, P.G., L.T. and A.S. All authors have read and agreed to the published version of the manuscript.

Funding: The research leading to these results has received funding from the Polish National Agency for Academic Exchange within the Bekker programme. The results are part of the project: Comparative assessment of enhanced geothermal systems with advanced exergy analysis, registration number PPN/BEK/2020/1/00310. The research leading to these results has received funding from the Norway Grants 2014–2021 via the National Centre for Research and Development. The results are part of the Polish-Norwegian project: CO_2-Enhanced Geothermal Systems for Climate Neutral Energy Supply, acronym EnerGizerS, registration number NOR/POLNOR/EnerGizerS/0036/2019.

Institutional Review Board Statement: Not applicable.

Informed Consent Statement: Not applicable.

Data Availability Statement: Not applicable.

Conflicts of Interest: The authors declare no conflict of interest.

Nomenclature

A	area (m^2)	P	pressure (Pa)
C	cost (EUR)	Q	heat (J)
CAPEX	capital expenditures	R	discount rate
CCS	carbon capture and storage	sCO_2	supercritical carbon dioxide
CO_2	carbon dioxide	T	temperature (°C)
d	depth (m)	W	power (W)
DHS	district heating system	U	heat transfer coefficient ($W/(m^2K)$)
E	electricity (J)	T	time (s, hr)
EGS	enhanced geothermal system		
f	factor	*Subscripts*	
HDR	hot dry rock		
H_2O	water	an	annual
LCOE	levelized cost of electricity	el	electrical
LCOH	levelized cost of heat	EQP	equipment
$\dot{m}$	mass flow rate (kg/s)	i	order parameter
n	project lifetime (yrs)	inj	injection
OPEX	operational expenditures	max	maximum
ORC	Organic Rankine Cycle	well	wellbore

References

1. European Commission. Commission Presents Renewable Energy Directive Revision. Available online: https://ec.europa.eu/info/news/commission-presents-renewable-energy-directive-revision-2021-jul-14_en (accessed on 20 July 2022).
2. Factsheets on Geothermal Electricity. Available online: http://www.geoelec.eu/wp-content/uploads/2011/09/All-Factsheets+-folder.pdf (accessed on 28 July 2022).
3. Lu, S.M. A Global Review of Enhanced Geothermal System (EGS). *Renew. Sustain. Energy Rev.* **2018**, *81*, 2902–2921. [CrossRef]
4. Huttrer, G.W. Geothermal Power Generation in the World 2015–2020 Update Report. In Proceedings of the World Geothermal Congress 2020+1, Reykjavik, Iceland, 24–27 October 2021; Available online: https://www.geothermal-energy.org/pdf/IGAstandard/WGC/2020/01017.pdf (accessed on 5 December 2022).
5. Raos, S.; Hranić, J.; Rajšl, I.; Bär, K. An Extended Methodology for Multi-Criteria Decision-Making Process Focused on Enhanced Geothermal Systems. *Energy Convers. Manag.* **2022**, *258*, 115253. [CrossRef]
6. European Commission. Technology Readiness Level: Guidance Principles for Renewable Energy Technologies. Final Report. 2017. Available online: https://op.europa.eu/en/publication-detail/-/publication/d5d8e9c8-e6d3-11e7-9749-01aa75ed71a1 (accessed on 24 October 2022).
7. United States Department of Energy, Office of Energy Efficiency and Renewable Energy. Funding Opportunity Exchange. Integrated Enhanced Geothermal Systems (EGS) Research and Development. Available online: https://eere-exchange.energy.gov (accessed on 25 October 2022).
8. Gładysz, P.; Sowiżdżał, A.; Miecznik, M.; Hacaga, M.; Pająk, L. Techno-Economic Assessment of a Combined Heat and Power Plant Integrated with Carbon Dioxide Removal Technology: A Case Study for Central Poland. *Energies* **2020**, *13*, 2841. [CrossRef]
9. Li, S.; Wang, S.; Tang, H. Stimulation Mechanism and Design of Enhanced Geothermal Systems: A Comprehensive Review. *Renewable and Sustainable Energy Rev.* **2022**, *155*, 111914. [CrossRef]
10. Haris, M.; Hou, M.Z.; Feng, W.; Mehmood, F.; bin Saleem, A. A Regenerative Enhanced Geothermal System for Heat and Electricity Production as Well as Energy Storage. *Renew. Energy* **2022**, *197*, 342–358. [CrossRef]
11. Zheng, S.; Li, S.; Zhang, D. Fluid and Heat Flow in Enhanced Geothermal Systems Considering Fracture Geometrical and Topological Complexities: An Extended Embedded Discrete Fracture Model. *Renew. Energy* **2021**, *179*, 163–178. [CrossRef]
12. Olasolo, P.; Juárez, M.C.; Morales, M.P.; Damico, S.; Liarte, I.A. Enhanced Geothermal Systems (EGS): A Review. *Renew. Sustain. Energy Rev.* **2016**, *56*, 133–144. [CrossRef]
13. Department of Energy. Enhanced Geothermal System (EGS) Fact Sheet. Available online: https://www.energy.gov/eere/geothermal/downloads/enhanced-geothermal-system-egs-fact-sheet (accessed on 20 October 2022).
14. Li, T.; Liu, Q.; Gao, X.; Meng, N.; Kong, X. Thermodynamic, Economic, and Environmental Performance Comparison of Typical Geothermal Power Generation Systems Driven by Hot Dry Rock. *Energy Rep.* **2022**, *8*, 2762–2777. [CrossRef]
15. Brown, D.W. A hot day rock geothermal energy concept utilizing super-critical CO_2 instead of water. In Proceedings of the Twenty-Fifth Workshop on Geothermal Reservoir Engineering, Stanford, CA, USA, 24–26 January 2000; Available online: https://pangea.stanford.edu/ERE/pdf/IGAstandard/SGW/2000/Brown.pdf (accessed on 29 June 2022).
16. Atrens, A.D.; Gurgenci, H.; Rudolph, V. Electricity Generation Using a Carbon-Dioxide Thermosiphon. *Geothermics* **2010**, *39*, 161–169. [CrossRef]

17. Schifflechner, C.; Dawo, F.; Eyerer, S.; Wieland, C.; Spliethoff, H. Thermodynamic Comparison of Direct Supercritical CO_2 and Indirect Brine-ORC Concepts for Geothermal Combined Heat and Power Generation. *Renew. Energy* **2020**, *161*, 1292–1302. [CrossRef]
18. White, M.T.; Bianchi, G.; Chai, L.; Tassou, S.A.; Sayma, A.I. Review of Supercritical CO_2 Technologies and Systems for Power Generation. *Appl. Therm. Eng.* **2021**, *185*, 116447. [CrossRef]
19. Saleh, B.; Koglbauer, G.; Wendland, M.; Fischer, J. Working Fluids for Low-Temperature Organic Rankine Cycles. *Energy* **2007**, *32*, 1210–1221. [CrossRef]
20. Heberle, F.; Brüggemann, D. Exergy Based Fluid Selection for a Geothermal Organic Rankine Cycle for Combined Heat and Power Generation. *Appl. Therm. Eng.* **2010**, *30*, 1326–1332. [CrossRef]
21. Quoilin, S.; van den Broek, M.; Declaye, S.; Dewallef, P.; Lemort, V. Techno-Economic Survey of Organic Rankine Cycle (ORC) Systems. *Renew. Sustain. Energy Rev.* **2013**, *22*, 168–186. [CrossRef]
22. Ungar, P.; Özcan, Z.; Manfrida, G.; Ekici, Ö.; Talluri, L. Off-Design Modelling of ORC Turbines for Geothermal Application. *Proc. E3S Web Conf.* **2021**, *312*, 11015.
23. Niknam, P.H.; Talluri, L.; Fiaschi, D.; Manfrida, G. Sensitivity Analysis and Dynamic Modelling of the Reinjection Process in a Binary Cycle Geothermal Power Plant of Larderello Area. *Energy* **2021**, *214*, 118869. [CrossRef]
24. Gładysz, P.; Sowiżdżał, A.; Miecznik, M.; Pająk, L. Carbon Dioxide-Enhanced Geothermal Systems for Heat and Electricity Production: Energy and Economic Analyses for Central Poland. *Energy Convers. Manag.* **2020**, *220*, 113142. [CrossRef]
25. Sarbu, I.; Mirza, M.; Muntean, D. Integration of Renewable Energy Sources into Low-Temperature District Heating Systems: A Review. *Energies* **2022**, *15*, 6523. [CrossRef]
26. Zhao, Q. Conception and Optimization of Supercritical CO_2 Brayton Cycles for Coal-Fired Power Plant Application. Ph.D. Thesis, Université de Lorraine, Lorraine, France, 2018.
27. Weiland, N.T.; Lance, B.W.; Pidaparti, S.R. sCO_2 Power Cycle Component Cost Correlations from DOE Data Spanning Multiple Scales and Applications. In *Proceedings of the ASME Turbo Expo 2019: Turbomachinery Technical Conference and Exposition*; Phoenix, AZ, USA, 17–21 June 2019. Available online: https://www.osti.gov/servlets/purl/1601743 (accessed on 24 July 2022).
28. Zhar, R.; Allouhi, A.; Jamil, A.; Lahrech, K. A Comparative Study and Sensitivity Analysis of Different ORC Configurations for Waste Heat Recovery. *Case Stud. Therm. Eng.* **2021**, *28*, 101608. [CrossRef]
29. Gładysz, P.; Saari, J.; Czarnowska, L. Thermo-Ecological Cost Analysis of Cogeneration and Polygeneration Energy Systems—Case Study for Thermal Conversion of Biomass. *Renew. Energy* **2020**, *145*, 1748–1760. [CrossRef]